Journal of Magnetism and Magnetic Materials 322 (2010) 2065–2070

Contents lists available at ScienceDirect

Journal of Magnetism and Magnetic Materials

journal homepage: www.elsevier.com/locate/jmmm

Spin-pumping-enhanced magnetic damping in ultrathin Cu(0 0 1)/Co/Cu and Cu(0 0 1)/Ni/Cu films

M. Charilaou *,[1], K. Lenz [2], W. Kuch

Institut für Experimentalphysik, Freie Universität Berlin, Arnimallee 14, 14195 Berlin, Germany

ARTICLE INFO

Article history:
Received 16 November 2009
Received in revised form
14 January 2010
Available online 25 January 2010

Keywords:
FMR
Ultrathin film
Spin torque effect
Magnetic relaxation

ABSTRACT

The influence of the Cu capping layer thickness on the spin pumping effect in ultrathin epitaxial Co and Ni films on Cu(0 0 1) was investigated by *in situ* ultrahigh vacuum ferromagnetic resonance. A pronounced increase in the linewidth is observed at the onset of spin pumping for capping layer thicknesses d_{Cu} larger than 5 ML, saturating at d_{Cu} = 20 ML for both systems. The spin mixing conductance for Co/Cu and Ni/Cu interfaces was evaluated.

© 2010 Elsevier B.V. All rights reserved.

1. Introduction

The structure and magnetic properties of ultrathin Cu(0 0 1)/Co/Cu and Cu(0 0 1)/Ni/Cu films have been studied extensively in past years [1–5]. Their tailorable magnetic performance makes such systems excellent candidates for fundamental investigations of magnetization dynamics. One of the most important features for the magnetic performance of devices for spintronics applications such as fast high density magnetic storage devices, spin valves, etc. [6], is the rate at which the magnetization can be switched, e.g. in order to write a bit of information. The magnetization dynamics in the ultrathin film regime, where the influence of bulk properties is eliminated, allows the direct observation of interfacial effects.

A precession of the magnetization in the ferromagnetic (FM) layer, i.e. Co or Ni, causes a spin current, which propagates through the interface into the nonmagnetic (NM) Cu substrate as well as into the cap layer, which act as spin sinks [7–10]. This spin pumping enhances the intrinsic relaxation of the magnetization in the FM layer, thus making switching processes faster.

FMR is a powerful method used for the determination of magnetic anisotropies and the characterization of magnetization dynamics. The utilization of FMR *in situ* in ultrahigh vacuum (UHV) allows for direct step-by-step preparation and measurement of the systems, which are thus characterized by high structural ordering and material purity, otherwise not achievable. In this work UHV FMR studies have been performed on single crystalline ultrathin Co and Ni films on Cu(0 0 1) with Cu cap layers of variable thickness, which are much thinner than the spin diffusion lengths of these systems [11]. In this thickness regime the interface-related relaxation mechanisms like spin-pump effect are dominant [12], especially at first contact between the vacuum side of the FM film and the NM cap layer.

The precessional motion of the magnetization vector $\vec{M}$, which for ferromagnetic films is regarded as a macro-spin, can be described by the Landau–Lifshitz–Gilbert (LLG) equation of motion [13,14]:

$$\frac{\partial \vec{M}}{\partial t} = -\gamma(\vec{M} \times \vec{H}_{\text{eff}}) + \frac{\alpha}{M_S}\left(\vec{M} \times \frac{\partial \vec{M}}{\partial t}\right), \tag{1}$$

where $\gamma = g\mu_B/\hbar$ is the gyromagnetic ratio, M_S the saturation magnetization. $\vec{H}_{\text{eff}}$ is the effective field including the external static field and the internal fields, i.e. anisotropy fields and microwave field, respectively. α is the dimensionless parameter of the intrinsic Gilbert damping, which depends on the strength of the spin–orbit coupling λ_{LS} : $\alpha \rightarrow \alpha_G \propto \lambda_{LS}^2$ [15]. Gilbert damping can be understood in terms of a viscous force, where the coupling of the spins to the orbital motion acts as a restoring force leading to a spiraling down of the spins toward the direction of the external field $\vec{H}_0$. This relaxation process is usually dominant in most cases and is called 'intrinsic'. However, in further examining the system the term 'intrinsic' looses its meaning at thicknesses where almost no volume contribution exists.

* Corresponding author.
E-mail address: michalis.charilaou@erdw.ethz.ch (M. Charilaou).
[1] New address: ETH Zurich, Institute of Geophysics, NO H11.3, Sonneggstrasse 5, CH-8092 Zurich, Switzerland.
[2] New address: Institute of Ion Beam Physics and Materials Research, Forschungszentrum Dresden-Rossendorf e.V., P.O. Box 51 01 19, 01314 Dresden, Germany.

0304-8853/$ - see front matter © 2010 Elsevier B.V. All rights reserved.
doi:10.1016/j.jmmm.2010.01.035

Other significant relaxation processes could be (i) eddy current damping, (ii) phonon dragging, and (iii) spin-pumping. (i) and (ii) can be neglected for ultrathin film systems since the damping amplitude depends on the thickness of the film $\alpha_{eddy} \propto d^2$ [16] and the phonon dragging contribution is an order of magnitude smaller than the Gilbert damping α_G [17,18]. Thus the only other significant additional contribution in this thickness range is spin pumping, which can be regarded as a Gilbert-like damping, since it has a similar mathematical form in the LLG [19]. Along the *in plane* easy axis the relation of the peak-to-peak linewidth ΔH_{pp} of the FMR signal to the microwave frequency is [20,21]

$$\Delta H_{pp} = \alpha_{eff} \frac{2}{\sqrt{3}} \frac{\omega}{\gamma} + \Delta H_{pp}^0, \tag{2}$$

where α_{eff} is the sum of contributions to the relaxation and ΔH_{pp}^0 is the contribution of inhomogeneities, which is constant for all frequencies and geometries. Furthermore, all films studied in this work were measured at 9 GHz. Prior *in situ* FMR experiments by Platow et al. on ultrathin Ni on a limited frequency range [22] give no indication for a two-magnon scattering contribution [23] to the damping. This leaves a total damping process involving only the Gilbert damping and spin-pumping:

$$\alpha_{eff} = \alpha_G + \alpha_{pump}. \tag{3}$$

However, note that two-magnon scattering would lead to an overestimation of α_{eff}. The study of the spin-pump effect on capped single films requires systems with well defined interfaces [12,24]. Cu/Co/Cu and Cu/Ni/Cu systems represent a good case for even interfaces due to the very small mismatch of the lattice constants, which is 1.9% for Co and 2.5% for Ni [25], and their pseudomorphic growth.

Precession of the magnetization vector around an effective field axis, like in FMR, is known to generate a spin current $\vec{I}_{pump}$, which flows from the FM layer into the NM layer [7]. If the NM layer is thick enough the spin current is dissipated there by spin-flip processes. Thus, torque is carried away from the precession and reduces the precessional energy of the FM layer. This process can be regarded as another damping mechanism. The contribution of spin pumping to the overall relaxation can be derived from the conservation of angular momentum in the FM layer [26,27]:

$$\frac{1}{\gamma}\frac{\partial \vec{\mu}_{tot}}{\partial t} = \vec{I}_{pump} \Rightarrow \frac{d\vec{m}}{dt} = \frac{\gamma}{M_S V}\vec{I}_{pump}, \tag{4}$$

where $\vec{\mu}_{tot} = \vec{m} M_S V$ is the total magnetic moment and $\vec{m}$ is the unit vector of magnetization. The spin current $\vec{I}_{pump}$ flowing through the FM/NM interface can be written as [7,19]

$$\vec{I}_{pump} = \frac{\hbar}{4\pi}\left[g_r^{\uparrow\downarrow}\left(\vec{m} \times \frac{d\vec{m}}{dt}\right) - g_i^{\uparrow\downarrow}\frac{d\vec{m}}{dt}\right], \tag{5}$$

where $g_r^{\uparrow\downarrow}$ is the real part of the spin mixing conductance $g^{\uparrow\downarrow}$. The imaginary part $g_i^{\uparrow\downarrow}$ can be neglected since $g_r^{\uparrow\downarrow} \gg g_i^{\uparrow\downarrow}$ [28–30]. Hence, inserting Eq. (5) into (4) results in

$$\frac{d\vec{m}}{dt} = \frac{\gamma}{M_S V}\frac{\hbar}{4\pi} g^{\uparrow\downarrow}\left(\vec{m} \times \frac{d\vec{m}}{dt}\right), \tag{6}$$

representing the additional loss of angular momentum from the FM layer. Adding the right hand side to the general LLG equation (1) rewritten in terms of the unit vector of magnetization yields

$$\frac{d\vec{m}}{dt} = -\gamma\left(\vec{m} \times \vec{H}_{eff}\right) + \underbrace{\left(\alpha_G + \frac{\gamma}{M_S V}\frac{\hbar}{4\pi} g^{\uparrow\downarrow}\right)}_{\alpha_{eff}}\left(\vec{m} \times \frac{d\vec{m}}{dt}\right). \tag{7}$$

Comparing Eqs. (3) and (7) one arrives at the expression for the spin-pumping contribution to the damping:

$$\alpha_{pump} = \frac{\gamma}{M_S V}\frac{\hbar}{4\pi} g^{\uparrow\downarrow} = \frac{g\mu_B}{4\pi M_S d_{FM}}\frac{g^{\uparrow\downarrow}}{S}, \tag{8}$$

where d_{FM} is the thickness of the ferromagnetic layer and S is the interface area.

This expression describes the damping caused by the total loss of spin energy transported by $\vec{I}_{pump}$, which is the case of having an ideal spin sink, i.e. no backflow due to spin accumulation in the NM cap layer. For a complete approach, one has to take this backflow $\vec{I}_{back}$ into account, which depends on $\vec{I}_{pump}$, the thickness of the NM cap layer d_{Cu}, and the spin diffusion length l_{sd} of about 350 nm in Cu at room temperature [11]. The net spin current $\vec{I}_{net} = \vec{I}_{pump} - \vec{I}_{back}$ equates to [12,29]

$$\vec{I}_{net} = \left[1 + \frac{\tau_{sf} g^{\uparrow\downarrow}}{hNSl_{sd}\tanh(d_{Cu}/l_{sd})}\right]^{-1}\vec{I}_{pump}, \tag{9}$$

where N is the density of states per spin and τ_{sf} the spin flip time. This can be expressed in terms of α_{pump} by comparing Eqs. (5), (6), and (8). Using N of a free electron gas, $N = (m_e k_F)/(2\pi^2\hbar^2)$ and $l_{sd} = \hbar k_F/m_e\sqrt{\tau_{el}\tau_{sf}/3}$, with the electron mass m_e, we arrive at a final expression for the damping parameter of the spin-pumping contribution:

$$\alpha_{pump} = \frac{g\mu_B}{4\pi M_S d_{FM}}\frac{g^{\uparrow\downarrow}}{S}\left[1 + \frac{\pi\sqrt{3}}{k_F^2\sqrt{\varepsilon}}\frac{g^{\uparrow\downarrow}}{S}\frac{1}{\tanh(d_{Cu}/l_{sd})}\right]^{-1}, \tag{10}$$

where $\varepsilon = \tau_{el}/\tau_{sf}$ is the spin flip probability per scattering event, with τ_{el} being the elastic scattering time, and k_F the Fermi wave vector, $k_F = \sqrt{2m_e E_F}/\hbar$ which is known to be $k_F = 1.36 \times 10^8\ \mathrm{cm}^{-1}$ for bulk Cu. The free parameters of this model are hence the conductance per unit area $g^{\uparrow\downarrow}/S$, the arbitrary spin flip probability ε and the spin diffusion length l_{sd}, which have been determined for this system, however, not been tested at length scales of a few monolayers and at first contact of a cap layer. Thus by measuring the FMR linewidth ΔH_{pp} of single uncapped Co and Ni films and gradually adding Cu we can calculate the change in α_{pump} using Eqs. (2) and (3) while assuming $\alpha_G = \text{const.}$, and determine the fit parameters for each system by applying the model in Eq. (10) for the thickness dependence.

2. Experimental details

The thin films examined in this work were grown *in situ* in UHV with a base pressure of 5×10^{-11} mbar on a Cu(0 0 1) single crystal disc, 5 mm in diameter and 2.5 mm thick. Prior to film deposition, the substrate was sputtered with Ar^+ ions at a partial pressure of 5×10^{-5} mbar with 3 keV for 10 min, then annealed at 850 K and sputtered again with 1 keV for another 10 min to smoothen the surface. After a final annealing again at 850 K for further 10 min, the Co (Ni) films with thicknesses of 1.6, 1.7, and 1.8 (6.0 and 7.0) monolayers (ML), respectively, were grown from high purity targets by means of electron beam evaporation. The optimum growth rate for all films was found to be 1 ML/min. The thickness was controlled during evaporation by means of medium energy electron diffraction (MEED). After deposition all films were annealed at 420 K for 10 min in order to smoothen the surface.

The Cu cover layers were prepared by the same procedure. However, no MEED signal could be detected for thicker films. Therefore, the thickness of the Cu cover layer was calculated according to the exposure time, based on a series of calibration runs on 10 ML thick Co films. The samples were annealed again at 420 K for 10 min after each additional Cu deposition step.

In situ FMR measurements were performed at 8.87 GHz using a cylindrical cavity with the TE_{012} mode. The cavity was mounted around the outside of a UHV quartz glass finger to the UHV chamber. This enables the measurement of FMR spectra *in situ* in UHV directly after preparation, hence without breaking the vacuum. Also it allows to change the thickness of the cap layer

by simply adding more Cu on top. Details of the UHV-FMR setup are described elsewhere [31,32].

3. Results and discussion

Single films were prepared and characterized as described in Section 2. Their anisotropy fields and effective magnetization $4\pi M_{\mathrm{eff}} = 4\pi M_S - 2K_{2\perp}/M_S$ were determined, before and after the deposition of the Cu cap layer, by means of polar angle-dependent FMR. An example is shown in Fig. 1, where the Co 1.8 ML and Ni 7.0 ML films are shown. The anisotropy fields were determined by fitting the angle dependence using an expression of the free energy density for tetragonally distorted systems in the polar resonance equation [32–34]. The effective magnetization of the Co films undergoes a large reduction from 13.6(1) kG, which is typical for thicknesses between 1.6 and 1.8 ML, down to 9.2(1) kG with a Cu cap layer above 5–10 ML thickness. The change of the effective magnetization in Ni films is more pronounced, here $4\pi M_{\mathrm{eff}}$ is reduced from 4.10(5) kG down to 1.00(5) kG. The Co films exhibit a fourfold in-plane anisotropy field $K_{4\parallel}/M$ of 30(5) G, which remains unchanged by Cu coverage. The effect of Cu coverage of ultrathin Co and Ni films on their magnetic anisotropy has been studied extensively (e.g. in Refs. [1,5,35,36]) and will therefore not be further examined here. For the study of the Cu thickness dependence on the resonance field and the linewidth of these films, FMR was measured at $\theta_B = 90^\circ$ along the [1 0 0] easy axis direction before and after step-by-step capping with 5 ML Cu each time at first and then with 10 ML. As can be seen in Fig. 2(a), the resonance field H_{Res} of the Cu(0 0 1)/x Co/d Cu films increases continuously with cap layer thickness and saturates at or before $d_{\mathrm{Cu}} \approx 20$ ML. The maximum relative increase in H_{Res} is 40–50% for all Co films. This large change is explained by the fact that the magnetic moment of the free surface of the Co atoms is reduced by the interaction with the electronic states of the adjacent Cu atoms. This interaction reduces the total magnetization by 21% [36], which according to the Landau–Lifshitz–Gilbert equation requires higher H_{Res}. For the Cu(0 0 1)/y Ni/d Cu films the change is even stronger (Fig. 3). The resonance field is shifted by 75% (7 ML) or 120% (6 ML) to higher values. This does not originate from a decrease in $\vec{M}$, since it has been found that the reduction of the Ni magnetic moment by a Cu cap compensates the former enhancement of a Ni/vacuum interface [35], and the contribution of volume atoms is much higher for the 6 ML and 7 ML Ni films than that of the interface atoms. The reason for this strong effect is the suppression of surface anisotropy of Ni, which favors in-plane orientation [2]. This is especially pronounced for those films with thicknesses just below the critical thickness for the spin reorientation transition [3].

The main effect of Cu capping takes place during the first 1–10 ML Cu. In order to determine the span of the interaction, we define a characteristic interaction depth d_{int} and fit the H_{Res} curves

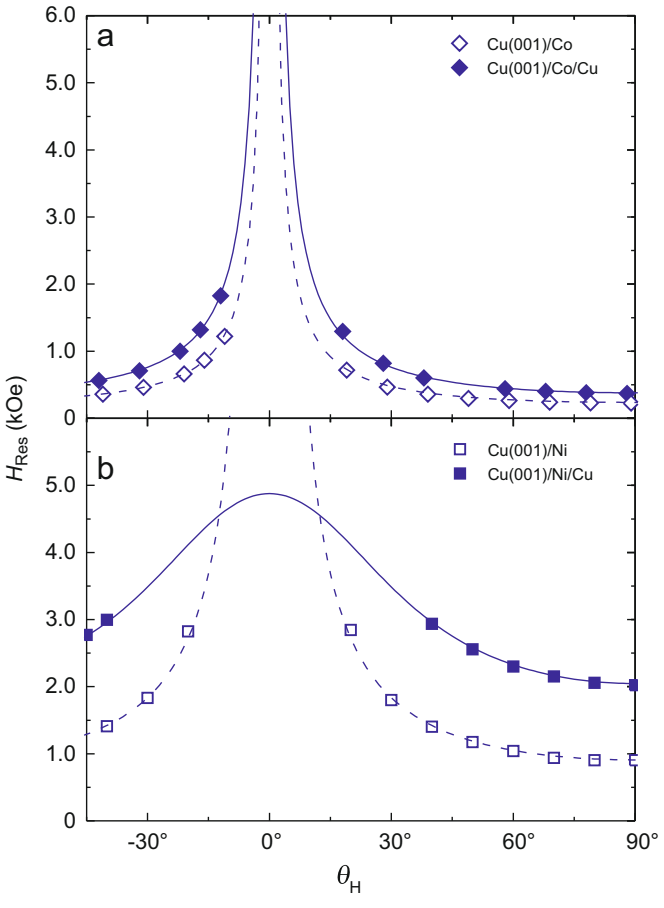

Fig. 1. Polar angular dependence of the resonance field H_{Res} at 8.87 GHz for (a) 1.8 ML Co and (b) 7.0 ML Ni before (open symbols) and after (solid symbols) deposition of a 25 ML Cu cap layer expressing the change in anisotropy. The solid lines are fits to the resonance equation for tetragonally distorted films given in Ref. [37].

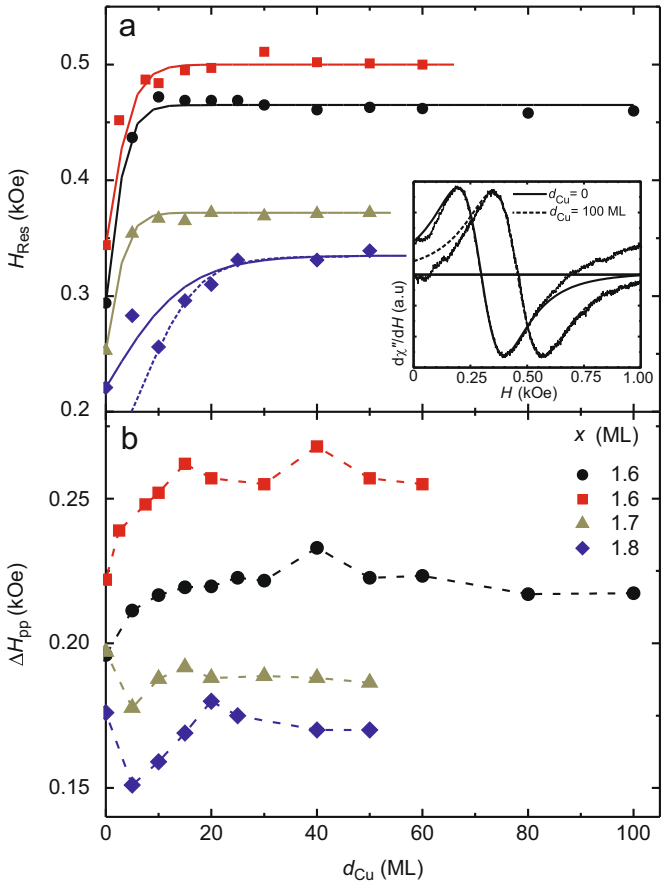

Fig. 2. (a) Resonance field H_{Res} of the Cu(0 0 1)/x Co/d_{Cu} Cu films as a function of Cu cap layer thickness d_{Cu}. The solid lines are fits with Eq. (11). The symbol size corresponds to the respective error in H_{Res}. The inset shows the resonance signal without (solid) and with (dashed) 100 ML Cu cap layer for x= 1.6 ML, where the lines are fits from first order Lorentzian derivatives. (b) Corresponding plot of the peak-to-peak linewidth ΔH_{pp}. Dashed lines are guides to the eye only.

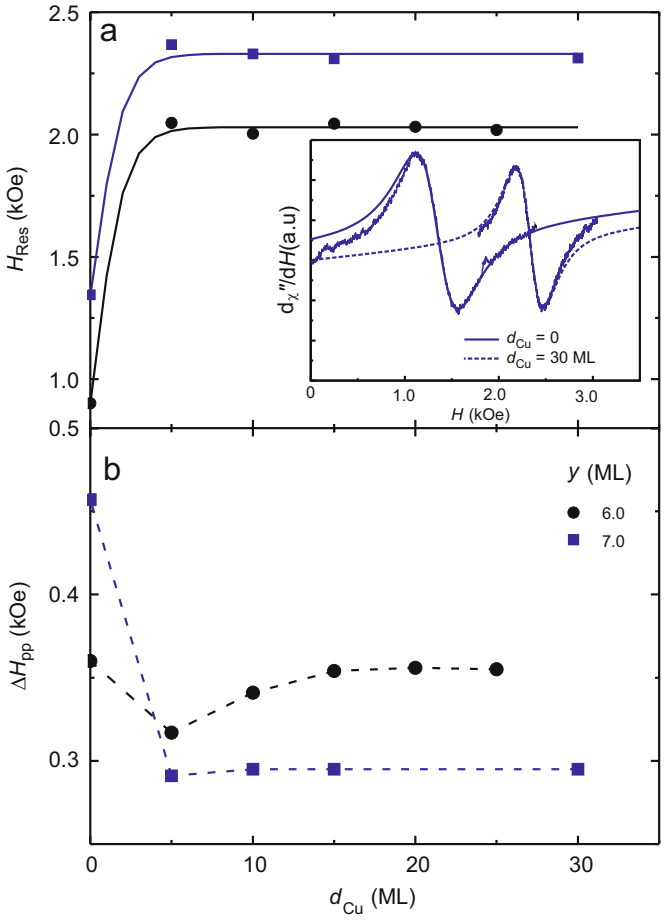

Fig. 3. (a) Resonance field H_{Res} of the Cu(0 0 1)/y Ni/d_{Cu} Cu films as a function of Cu cap layer thickness d_{Cu}. The solid lines are fits with Eq. (11). The inset shows the resonance signal without (solid) and with (dashed) 30 ML Cu cap layer for y = 7.0 ML. The fits are first order Lorentzian derivatives. (b) Corresponding plot of the peak-to-peak linewidth ΔH_{pp}. Dashed lines are guides to the eye only.

with a purely phenomenological saturating function

$$H_{Res} = \Delta H_{Res} \tanh\left(\frac{d_{Cu}}{d_{int}}\right) + H^0_{Res}, \quad (11)$$

where H^0_{Res} is the initial value and ΔH_{Res} the total increase of the resonance field. The interaction depths d_{int} were found to be 5 ML for the Co films with thicknesses 1.6 and 1.7 ML, and 15 ML for 1.8 ML. The value of d_{int} for the thicker film is much larger, since the surface tends to coalesce when approaching a full 2 ML. For a closed surface the effect is expected to be more pronounced, since a smoother interface will create a smaller Coulomb 2-D field, hence the FM film will be more easily affected by superimposed potentials of neighboring Cu atoms. Furthermore, the resonance field of the 1.8 ML film exhibits a small local maximum as seen in Fig. 2(a) between d_{Cu}=0 and 10 ML. This curve can be also fitted with an offset of 5 ML Cu (dashed line), which yields d_{int}=10 ML. For all Ni films the interaction depth is much smaller and was found to be 2 ML, which is in agreement with results from Nakagawa et al. [2]. This can be explained by the roughness at the interface. A strong potential barrier is formed at the interface, which dominates over the effect of the following Cu layers. The extracted interaction depth d_{int} is important for the determination of the onset of equilibrium in anisotropy and intrinsic damping α_G as will be explained later on.

The insets in Figs. 2 and 3 show the FMR signals taken for uncapped and capped films. These exhibit a symmetric Lorentzian line shape and can be fitted with a first order derivative [38], allowing the determination of the linewidth with an accuracy of 2–3%. Hence, using Eq. (2), the enhanced damping α_{eff} can be calculated from the linewidth. As seen in Fig. 2(b), Co films with a thickness of 1.6 ML exhibit an increase up to $d_{Cu} \approx 20$ ML with two small maxima at 15 and 40 ML Cu. Films with thicknesses 1.7 ML and 1.8 ML show an abrupt fall and a gradual increase approximating that of the 1.6 ML films. This makes the calculations for the spin current extremely complicated since many effects may take place at the same time during the transition from d_{Cu}=0 to d_{Cu}=d_{int}: (i) The surface/interface magnetic moment is reduced. (ii) The anisotropies and the equilibrium angles change. (iii) The spin–orbit interaction of the Co and Ni interface atoms is reduced by the presence of the Cu d-orbitals. Hence α_G is also reduced during the first 5 ML of Cu capping, as α_G is proportional to the square of the spin–orbit coupling constant as mentioned earlier. This change is dominant over this region and cannot be determined directly. Therefore, one has to consider the interaction depth as determined using Eq. (11). Thus the pure spin pumping contribution can be calculated only for $d_{Cu} \geq d_{int}$, where $\alpha_G = \text{const}$.

The dimensionless damping constant α_{pump} was evaluated by determining α_{eff} using Eq. (2) and subtracting the value at d_{int}. The increase in α_{pump} was then fitted as described in Section 1 using Eq. (10). The values of M_S are taken from [36] for Co and from [35] for Ni, which are given for T = 0 K, and were extrapolated to room temperature considering the reduced temperature T/T_C, as 800 G for Co and 450 G for Ni films. For both film series the spectroscopic factor g=2.20 was used. The result for the two samples with 1.6 ML Co is shown in Fig. 4. The data of the two 1.6 ML Co films can be fitted nicely using Eq. (10) except for the two maxima at 15 ML and 40 ML, and for data points at large Cu thicknesses, where the relaxation decreases slightly. All films were fitted for $d_{Cu} \geq 5$ ML. The fits of the other samples are shown in Fig. 5, which show that the model can be approximated to the experimental data with only small deviations. The corresponding fit parameters are listed in Table 1. Both the 1.6 ML Co films show an increase in α_{eff} from the beginning, which however cannot be thought of as pure spin-pump damping considering the changes in the resonance field. By fitting the data from d_{Cu}=0 ML thus assuming pure spin-pumping we acquire a value for the mixing conductance of 2.0(1) × 10^{15} cm^{-2}, which is almost 4 times larger

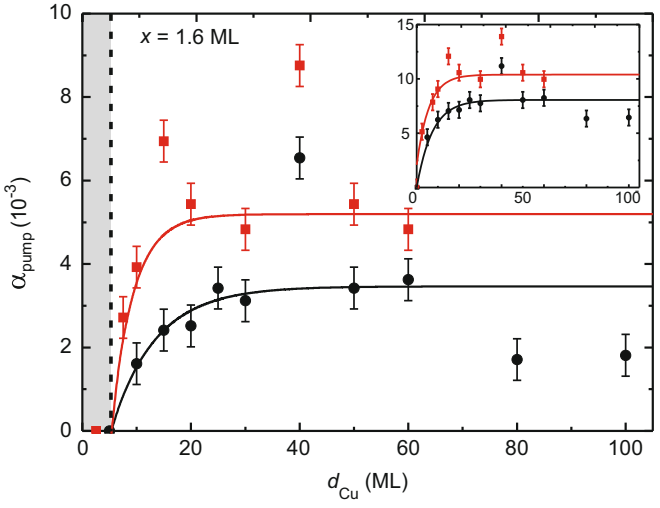

Fig. 4. Spin-pump damping parameter α_{pump} of the two 1.6 ML Co films as a function of the thickness of the Cu cap layer d_{Cu}. The solid lines are fits calculated using Eq. (10). The error bars are approximations considering the evaluation of α from ΔH_{pp}. The fit parameters are given in Table 1. The inset shows a fit starting at d_{Cu}=0.

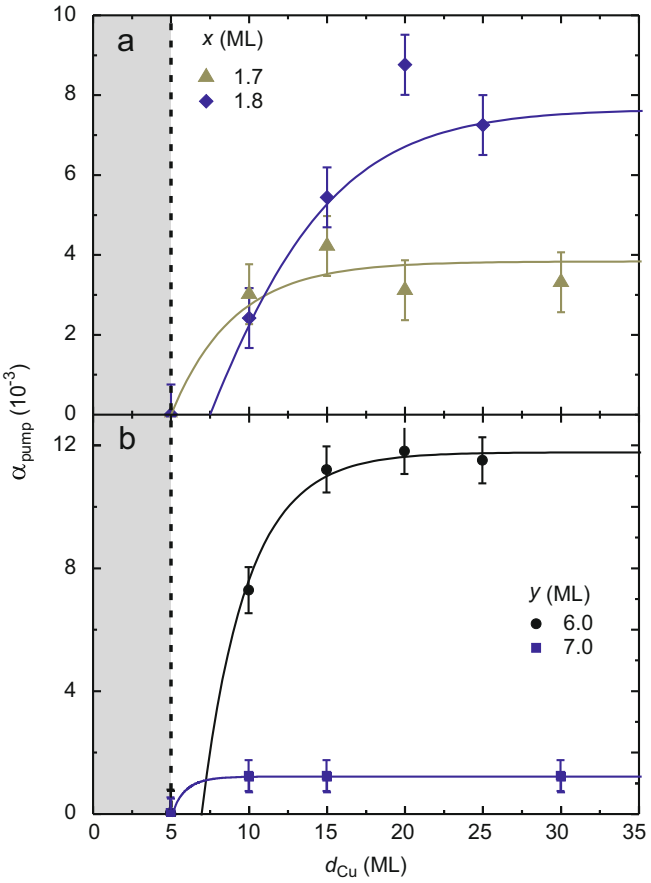

Fig. 5. Spin-pump damping α_{pump} of (a) 1.7 ML Co (triangles) and 1.8 ML Co (diamonds) and (b) 6 ML Ni (circles) and 7.0 ML Ni (squares) as a function of the cap layer thickness d_{Cu}. Solid lines represent fits using Eq. (10). For the shaded area ($d_{Cu} \leq 5$ ML) α_{pump} cannot be extracted since $\alpha_{pump} \neq \alpha_{tot} - \alpha_G$. The error bars are approximations considering calculation of α from ΔH_{pp}. The fit parameters are presented in Table 1.

Table 1
Total spin-pump damping α^{tot}_{pump}, maximum change of the intrinsic Gilbert damping $\Delta\alpha_G$ during deposition of the first five ML of Cu, and fit parameters for the spin-pump damping contribution for Cu(0 0 1)/x Co/d_{Cu} Cu and Cu(0 0 1)/y Ni/d_{Cu} Cu films.

x (ML)	α^{tot}_{pump} (10^{-3})	$\Delta\alpha_G$ (10^{-3})	$g^{\uparrow\downarrow}/S$ (10^{15} cm $^{-2}$)	l_{sd} (ML)	ε (10^{-3})
1.6	5.2(2)	5.1(2)	0.225(5)	6(1)	1.0
1.6	3.3(2)	4.6(2)	0.085(2)	16(2)	1.0
1.7	3.4(5)	−5.8(2)	0.125(2)	9(1)	1.0
1.8	7(1)	−7.5(2)	0.550(5)	13(2)	2.1
y (ML)					
6.0	11.1(3)	−12.0(5)	4.0(1)	6.0(5)	12.5
7.0	1.1(2)	−50(1)	0.075(2)	2.0(5)	1.0

than expected. This is an indication of the validity of the 5 ML limitation for the calculations. When fitted from d_{int}, the fitting yields an average over the two 1.6 ML films of $g^{\uparrow\downarrow}/S = 0.16(1) \times 10^{15}$ cm^{-2} which is in reasonable agreement with theoretical values given in Ref. [39], where it was found to be 0.55×10^{15} cm^{-2}, after it was corrected down from 1.1×10^{15} cm^{-2} in an earlier study [40].

The Co films with x_{Co}=1.7 and 1.8 ML show a clear increase in the damping constant above d_{Cu}=5 ML. The fit for the 1.8 ML film yields a very high value for $g^{\uparrow\downarrow}/S$, which is twice as large as the ones for 1.6 and 1.7 ML. Since the value for $g^{\uparrow\downarrow}/S$ should not exceed the theoretical upper limit the data for this film were fitted with a larger spin flip probability of 2.1×10^{-3}. The film also exhibits the greatest reduction of intrinsic damping $\Delta\alpha_G = -7.5 \times 10^{-3}$ upon deposition of the first five ML of Cu.

The two maxima at 15 ML and 40 ML cannot be explained by the current model. They are equidistant with respect to zero, within the error for d_{Cu}, thus we suspect an oscillatory behavior with a periodicity of 20(5) ML. Such a maximum can also be seen for the 1.8 ML Co film for d_{Cu}=20 ML. These oscillations would confirm predictions in Ref. [41], where short and long period oscillations are suggested to be caused by quantum size effects, in which the wave vector perpendicular to the interface is not conserved. The data are not enough to fit an oscillatory behavior as proposed in [41], however the reproducibility in the two 1.6 ML films points to the validity of the theory.

The 6 ML Ni film exhibits an astonishingly high value of $g^{\uparrow\downarrow}/S = 4.0(1) \times 10^{15}$ cm^{-2}, whereas the 7 ML film shows spin pumping with $0.075(2) \times 10^{15}$ cm^{-2} comparable to the Co films. It has been reported that the spin mixing conductance of Cu/Ni/Cu interfaces exhibits an oscillatory behavior with a period of 10 ML Ni [42]. This however does not explain the large difference between the two Ni films. The strongly reduced spin mixing conductance of the 7 ML film is most probably due to the rough interface, since it is known that Ni starts growing in island mode above 5–6 ML, as was reported in [43] and seen by MEED by ourselves where intensity oscillations are visible only up to 5–7 ML Ni. We have no reference values for the Ni films to compare with since to our knowledge spin pumping in Cu/Ni/Cu systems has not been measured before.

The spin flip probability ε was set to 0.001 for all films, except Co 1.8 ML and Ni 6.0 ML. This was done with respect to theoretical values of ε for Cu [44–46]. The general deviation from the theoretical values is the sensitivity of $g^{\uparrow\downarrow}/S$ to the interface smoothness, which cannot be fully controlled with uncompleted layers like the ones for Co, and the choice of ε, where a factor of 10 affects $g^{\uparrow\downarrow}/S$ by a factor of 2–3. This creates a distribution of spin channel conductivity values. Supposing that each interface atom constitutes a spin channel, good contacts correspond to open spin channels, whereas distorted lattice locations correspond to partly blocked channels with reduced conductivity. Although the values for $g^{\uparrow\downarrow}/S$ for Co would be expected to be the same, it has to be taken into consideration that—to the knowledge of the authors—the model has not yet been tested in this thickness regime, where the spin-pumping is just starting. The error bars shown in Figs. 4 and 5 originate from the assumption that no ΔH^0_{pp} is present. This suggests a relative error of less than 10%. The error of the spin mixing conductance coefficient $g^{\uparrow\downarrow}/S$ is mostly determined by the error in the film magnetization, as ε was assigned a fixed value for fitting.

Furthermore the characteristic length for spin diffusion l_{sd} was found to be between 9 and 15 ML for all Co films, which is much less than the known 350 nm ($\approx$1900 ML) [11]. At these length scales we would have expected an almost linear behavior considering $\tanh(d_{Cu}/l_{sd}) \approx d_{Cu}/l_{sd}$. The dominant interface 'shock' effects, where the first contact between Co (Ni) and Cu atomic layers takes place, creates an abrupt electronic perturbation which corresponds to a singularity at the interface. Hence the length found in our fits is not the spin diffusion length in its sense, rather the span of the scattering potential of the Co/Cu interface, which is comparable to the interaction depths determined for the magnetization reduction. The fact that the effect saturates at these length scales suggests that the model for non-local damping with the transport theory approach is not valid for atomic-scale systems.

4. Conclusions

We have prepared Cu/Co/Cu and Cu/Ni/Cu ultrathin films *in situ* in UHV and measured FMR in order to study spin pumping at thicknesses well below the spin diffusion length, which allowed us to probe interfacial effects during first contact of Co (Ni) and Cu atomic layers. The resonance field H_{Res} of all films increased with increasing Cu cap thickness d_{Cu} up to a saturating point around 20 ML Cu. The FMR linewidth was used to calculate the damping coefficient $\alpha_{eff} = \alpha_G + \alpha_{pump}$. Spin pumping was observed for all films. This was especially pronounced for the two Cu(0 0 1)/ 1.6 Co/d_{Cu} Cu films where the damping constant α_{eff} increased up to a saturating value of 15–20% of the initial α_G. For all other films the abrupt decrease in linewidth was caused by a strong reduction of α_G at the Co/Cu interface. However, this effect saturated after 5 ML Cu, while spin-pumping was observed after adding more Cu layers. This sets the limitation for the calculation of pure spin pumping within this interval. We used a model derived from a transport theory approach [29] to extract values for the spin mixing conductance $g^{\uparrow\downarrow}/S$. There values are in reasonable agreement with theoretical values for Cu/Co interfaces, however, the ones for Cu/Ni films are very high. Considering the fitting results, we conclude that the model is not appropriate for the system at these length scales. For atomic-scale systems a model, in which the first contact between FM and NM layers is considered would be more appropriate. We deduce from our results that at the starting point of spin-pumping, scattering events at the FM/NM interface govern the relaxation process in ultrathin films.

References

[1] M.E. Buckley, F.O. Schumann, J.A.C. Bland, Phys. Rev. B 52 (1995) 6596; M.E. Buckley, F.O. Schumann, J.A.C. Bland, J. Phys. Condens. Matter. 8 (1996) L147.
[2] T. Nakagawa, H. Watanabe, T. Yokoyama, Surf. Sci. 599 (2005) 262.
[3] W.L. O'Brien, T. Droubay, B.P. Tonner, Phys. Rev. B 54 (1996) 9197.
[4] G. Bochi, C.A. Ballentine, H.E. Inglefield, C.V. Thompson, R.C. O' Handley, Phys. Rev. B 53 (1996) R1729.
[5] V.I. Gavrilenko, R. Wu, Phys. Rev. B 60 (1999) 9539; V.I. Gavrilenko, R. Wu, J. Appl. Phys. 87 (2000) 6098.
[6] A. Brataas, Y. Tserkovnyak, G.E.W. Bauer, B.I. Halperin, Phys. Rev. B 66 (2002) 060404(R).
[7] Y. Tserkovnyak, A. Brataas, G.E.W. Bauer, Phys. Rev. Lett. 88 (2002) 117601.
[8] B. Heinrich, R. Urban, G. Woltersdorf, IEEE Trans. Magn. 38 (2002) 2496.
[9] M. Stiles, A. Zangwill, Phys. Rev. B 66 (2002) 014407.
[10] K. Lenz, T. Toliński, J. Lindner, E. Kosubek, K. Baberschke, Phys. Rev. B 69 (2004) 144422.
[11] F.J. Jedema, A.T. Filip, B.J. van Wees, Nature 410 (2001) 345.
[12] R. Urban, B. Heinrich, G. Woltersdorf, J. Appl. Phys. 93 (1993) 8280.
[13] L. Landau, E. Lifshitz, Phys. Z. Sowjetunion. 8 (1935) 153.
[14] T.L. Gilbert, IEEE Trans. Magn. 40 (2004) 3443.
[15] V. Kamberský, Can. J. Phys. 48 (1970) 2906.
[16] J.A.C. Bland, B. Heinrich, Ultrathin Magnetic Structures IV, Springer, Berlin, Heidelberg, New York, 2005.
[17] H. Suhl, IEEE Trans. Magn. 34 (1998) 1834.
[18] B. Heinrich, J.F. Cochran, K. Myrtle, J. Appl. Phys. 53 (1982) 2092.
[19] O. Mosendz, G. Woltersdorf, B. Kardaz, B. Heinrich, C.H. Back, Phys. Rev. B 79 (2009) 224412.
[20] H. Suhl, Phys. Rev. 97 (1955) 555.
[21] S.V. Vonsovskii, Ferromagnetic Resonance, Pergamon, Oxford, 1966.
[22] W. Platow, A.N. Anisimov, G.L. Dunifer, M. Farle, K. Baberschke, Phys. Rev. B 58 (1998) 5611.
[23] K. Lenz, H. Wende, W. Kuch, K. Baberschke, K. Nagy, A. Janossy, Phys. Rev. B 73 (2006) 144424.
[24] A. Brataas, Y.V. Nazarov, G.E.W. Bauer, Eur. Phys. J. B 22 (2001) 99.
[25] L. Börnstein, New Series Group III: Condensed Matter, Physics of Solid Surfaces III/24, Springer, Berlin, 1993.
[26] L. Berger, Phys. Rev. B 54 (1996) 9353.
[27] L. Berger, Phys. Rev. B 79 (1999) 11465.
[28] K. Xia, P.J. Kelly, G.E.W. Bauer, I. Turek, J. Kurdnovský, V. Drchal, Phys. Rev. B 63 (2001) 064407.
[29] Y. Tserkovnyak, A. Brataas, G.E.W. Bauer, Phys. Rev. B 66 (2002) 224403.
[30] Y. Tserkovnyak, A. Brataas, G.E.W. Bauer, Phys. Rev. B 67 (2003) 140404(R).
[31] M. Farle, Rep. Prog. Phys. 61 (1998) 755.
[32] J. Lindner, K. Baberschke, J. Phys. Condens. Matter 15 (2003) R193.
[33] L. Beselgia, M. Warden, F. Waldner, S.L. Hutton, J.E. Drumheller, Y.Q. He, P.E. Wigen, M. Marysko, Phys. Rev. B 38 (1988) 2237.
[34] J. Smit, H.G. Beljers, Philips Res. Rep. 10 (1955) 113.
[35] A. Ney, A. Scherz, P. Poulopoulos, K. Lenz, H. Wende, K. Baberschke, Phys. Rev. B 65 (2001) 024411.
[36] A. Ney, P. Poulopoulos, K. Baberschke, Europhys. Lett. 54 (2001) 820.
[37] K. Lenz, E. Kosubek, K. Baberschke, H. Wende, J. Herfort, H.-P. Schönherr, K.H. Ploog, Phys. Rev. B 72 (2005) 144411.
[38] C.P. Poole Jr., Electron Spin Resonance: A Comprehensive Treatise on Experimental Techniques, Interscience Publishers, New York, 1967.
[39] Y. Tserkovnyak, A. Brataas, G.E.W. Bauer, B.I. Halperin, Rev. Mod. Phys. 77 (2005) 1375.
[40] K. Xia, J.P. Kelly, G.E.W. Bauer, A. Brataas, I. Turek, Phys. Rev. B 65 (2002) 220401R.
[41] D.L. Mills, Phys. Rev. B 68 (2003) 014419.
[42] I. Turek, K. Carva, Acta Phys. Pol. A 113 (2008) 11.
[43] P. Poulopoulos, J. Lindner, M. Farle, K. Baberschke, Surf. Sci. 437 (1999) 277.
[44] R. Meservey, P.M. Tedrow, Phys. Rev. Lett. 41 (1978) 805.
[45] G. Bergmann, Z. Phys. B Condens. Matter 48 (1982).
[46] Q. Yang, P. Holody, S.-F. Lee, L.L. Henry, R. Loloee, P.A. Schroeder, W.P. Pratt, J. Bass, Phys. Rev. Lett. 72 (1994) 3274.